

The serine/threonine kinase Back seat driver prevents cell fusion to maintain cell identity

Shuo Yang¹ and Aaron N. Johnson^{1,2}

¹Department of Developmental Biology
Washington University School of Medicine
St. Louis, MO 63110

²Author for correspondence: anjohnson@wustl.edu
Running Title: Bsd maintains cell identity

Keywords: cell identity, muscle development, myoblast fusion, Bsd

1 **Abstract**

2 Cell fate specification is essential for every major event of embryogenesis, and
3 subsequent cell maturation ensures individual cell types acquire specialized functions. The
4 mechanisms that regulate cell fate specification have been studied exhaustively, and each
5 technological advance in developmental biology ushers in a new era of studies aimed at
6 uncovering the most fundamental processes by which cells acquire unique identities. What is
7 less appreciated is that mechanisms are in place to ensure cell identity is maintained throughout
8 the life of the organism. The body wall musculature in the *Drosophila* embryo is a well-
9 established model to study cell fate specification, as each hemisegment in the embryo
10 generates and maintains thirty muscles with distinct identities. Here we show the
11 serine/threonine kinase Back seat driver (Bsd), which regulates muscle morphogenesis, also
12 maintains cell identity. Once specified, the thirty body wall muscles fuse with mononucleate
13 muscle precursors that lack a specific identity to form multinucleate striated muscles.
14 Importantly, body wall muscles do not fuse with each other and thereby maintain distinct
15 identities. We show that Bsd prevents inappropriate fusion among the thirty body wall muscles.
16 Thus, the regulation of cell fusion is one mechanism that maintains cell identity.

17 Introduction

18 Cell fate specification is a hallmark of embryonic development, and as development
19 proceeds fated cells mature and acquire specialized identities and functions. Our understanding
20 of cell fate specification was revolutionized by the gene regulatory network (GRN) hypothesis in
21 which extracellular signals regulate the expression of transcription factors that in turn regulate
22 gene expression via *cis*-regulatory modules in the network, establish cell identity, and ultimately
23 activate expression of the structural genes that perform specialized functions (Peter and
24 Davidson, 2016). Cell identity is intimately connected to the overall body plan. Once cells
25 acquire identity and specialized functions, cell identity must be maintained for the organism to
26 operate at the selected capacity. One mechanism that promotes the stability of cell identity
27 involves epigenome regulated changes in the accessibility of chromatin to transcription factors
28 (Balsalobre and Drouin, 2022). However, the genomes of neighboring cells must remain
29 isolated for epigenomics to maintain cell identity.

30 After gastrulation, the *Drosophila* mesoderm subdivides into the cardiac, visceral and
31 somatic mesoderm; the somatic mesoderm will give rise to the striated body wall muscles.
32 Thirty distinct body wall muscles develop per hemisegment, and each muscle expresses a
33 distinct set of transcription factors that confers a unique cell identity. The diversification of body
34 wall muscle cell types initiates when Wingless and Decapentaplegic signals establish
35 competence domains in the somatic mesoderm (Carmena et al., 1998). Cells in each domain
36 are competent to respond to subsequent Receptor Tyrosine Kinase signals, which refine the
37 competence domain to a smaller group of equivalent cells. Lateral inhibition within the
38 equivalence group selects a single progenitor to become a founder cell (FC). The remaining
39 cells in the equivalence group will become fusion competent myoblasts (FCMs). Altogether,
40 thirty FCs are specified per hemisegment and each FC acquires a unique identity through the
41 expression of transcription factors known as identity genes (de Jossineau et al., 2012;
42 Sandmann et al., 2006). FCs directionally fuse with FCMs to generate multinucleate myotubes,
43 but FCs will not fuse with each other (Bothe and Baylies, 2016). At the completion of
44 myogenesis, the thirty FCs will have generated thirty body wall muscles with distinct identities,
45 morphologies, and intrasegmental positions. Although the mechanisms that direct FC
46 diversification have been studied in detail, it is unclear how directional myoblast fusion is
47 regulated so that muscle cell identity is maintained.

48 Here we report that the serine/threonine kinase Back seat driver (Bsd) regulates
49 directional fusion to stabilize muscle cell identity. Live imaging studies revealed multinucleate
50 myotubes derived from distinct FCs fuse with each other in the absence of Bsd activity. We

51 have previously shown that Bsd and the Rho GTPase Tumbleweed (Tum) function in a common
52 pathway to regulate muscle morphogenesis, but Tum does not appear to regulate directional
53 fusion. Instead Bsd regulates Mitogen Activated Protein Kinase (MAPK) activity, which may be a
54 mechanism for limiting non-directional muscle fusion. Interestingly, the transcription factor
55 Jumeau (Jumu) regulates both cell fate specification and chromatin remodeling, and we found
56 Jumu also activates Bsd expression. Our studies suggest that, in addition to epigenetic
57 regulation, Jumu maintains cell identity by preventing cell-cell fusion through a Bsd-dependent
58 mechanism.

59 Results and Discussion

60 Founder cells (FCs) begin to elongate just after specification, and concurrently initiate
61 directional fusion with neighboring fusion competent myoblasts (FCMs) to form syncytial
62 myotubes (Bothe and Baylies, 2016). The nascent myotube leading edges will navigate across
63 the hemisegment and identify muscle attachment sites on tendon cells in the ectoderm.
64 Myotube guidance refers to the combined processes of leading edge navigation and muscle
65 attachment selection, and regulated myotube guidance establishes a stereotypical
66 musculoskeletal pattern in abdominal segments A2-A8 (Figure 1A). We identified Back seat
67 driver (Bsd) in a previous study of myogenesis, and found Bsd is an essential regulator of
68 myotube guidance (Yang et al., 2020).

69 Each FC expresses a unique set of transcription factors known as identity genes.
70 Enhancers from the identity gene *slouch* (*slou*) were used to generate a transgenic reporter
71 gene (*slou-CD8-GFP*), which is active in six FCs that give rise to the Dorsal Transverse 1 (DT1),
72 the Longitudinal Oblique 1 (LO1), Ventral Acute 1-3 (VA1-3), and the Ventral Transverse 1
73 (VT1) muscles (Figure 1A)(Schnorrer et al., 2007). A transgenic *Gal4* line constructed from
74 similar *slou* enhancers (*slou.Gal4*) recapitulates the activity of the *slou-CD8-GFP* reporter (Yang
75 et al., 2020). Enhancers from the identity gene *nautilus* (*nau*) comprise a third transgenic line
76 (*nau.Gal4*), which is active in the Dorsal Oblique 3 (DO3), Longitudinal Lateral 1 (LL1), Ventral
77 Lateral 1 (VL1), and Ventral Oblique 4-5 (VO4-5; Fig. 1A)(McAdow et al., 2022). *slou-CD8-GFP*
78 and *nau.Gal4* are active in non-overlapping populations of body wall muscles, and in wild-type
79 embryos *slou-CD8-GFP* and *nau.Gal4*, *UAS.tdTomato* (*nau>tdTom*) were rarely co-expressed
80 in body wall muscles (Fig. 1B,C). Surprisingly the number of muscles that co-expressed *slou-*
81 *CD8-GFP* and *nau>tdTom* in *bsd¹* embryos was significantly greater than controls (Fig. 1B,C).
82 These data suggest *bsd¹* muscles adopt abnormal identities.

83 FCs are correctly specified in *bsd¹* embryos (Yang et al., 2022), so we used live imaging
84 to understand how Bsd might regulate muscle identity. Nascent myotubes extend bipolar
85 projections to connect with muscle attachment sites that link muscles to the exoskeleton (Fig.
86 1D, Supplementary Movie 1). During elongation, LO1 myotubes that expressed *slou>GFP* fused
87 with FCMs but not with other myotubes that expressed *slou>GFP* (Fig. 1E). In contrast, 28% of
88 LO1 myotubes in *bsd¹* embryos fused with neighboring *slou>GFP* myotubes (Fig 1D,E), arguing
89 Bsd prevents non-directional fusion between myotubes to maintain cell identity.

90 Bsd directly activates Polo kinase, and active Polo in turn regulates many downstream
91 effectors, including the GTPase activating protein Tumbleweed (Tum) and the kinesin
92 microtubule motor protein Pavarotti (Pav) (D'Avino et al., 2006; Ebrahimi et al., 2010; Gregory et

93 al., 2008; Somers and Saint, 2003). Polo, Tum, and Pav act in a common myogenic pathway to
94 direct myotube guidance (Guerin and Kramer, 2009; Yang et al., 2022), so we asked if Bsd acts
95 through the Polo/Tum/Pav cytoskeletal regulatory module to maintain direction fusion. *tum*^{DH15}
96 produced the strongest muscle phenotypes among the *polo*, *pav*, and *tum* alleles we tested
97 (Yang et al., 2022) and, while live imaging showed *tum*^{DH15} embryos have highly penetrant
98 myotube guidance defects, we did not observe any instances of LO1 myotubes fusing with
99 neighboring *slou>GFP* myotubes (Fig 2A,B; Supplementary Movie 2). These live imaging
100 studies argue Bsd acts through a Polo/Tum/Pav independent pathway to regulate cell fusion.

101 In *Drosophila* visceral muscles, Anaplastic lymphoma kinase (Alk) activates extracellular
102 signal-regulated kinase (ERK) to induce the expression of the cell adhesion molecule Kirre,
103 which is essential for myoblast fusion (Englund et al., 2003; Krauss, 2010). In contrast, the Bsd
104 orthologue Vaccinia-related kinase 3 (VRK3) inactivates ERK by regulating the ERK
105 phosphatase Vaccinia H1-related (Kang and Kim, 2006, 2008). One possibility is that Bsd
106 inactivates ERK in *Drosophila* to suppress Kirre expression, and in turn regulate cell fusion. We
107 assayed phosphorylated ERK (dpERK) *in vivo* and *in vitro*, and found *bsd*¹ embryos had
108 significantly more dpERK than control embryos (Fig. 2C-E), and S2 cells transfected with Bsd
109 had significantly less phosphorylated ERK than control transfected cells (Fig. 2F). These results
110 are consistent with the hypothesis that Bsd inactivates ERK to regulate cell fusion. Although a
111 Kirre antibody is no longer available, our studies suggest that ERK-regulated pathways control
112 Kirre expression in body wall muscles to direct myoblast fusion.

113 We next asked what pathways might be regulating Bsd to ensure muscle cell identity is
114 correctly maintained. Using mass spectrometry, we identified a number of proteins that
115 physically interact with Bsd, including Polo, but none of the candidates are known regulators of
116 myogenesis (Yang et al., 2022). Regulatory kinases are differentially expressed during
117 organogenesis (Yang et al., 2022), so we used the DNAMAN prediction tool to identify
118 transcription factor binding sites near the *bsd* locus. *bsd* transcription is controlled by two core
119 promoters, and each promoter is less than 400bp from a consensus binding site for the
120 transcription factor Jumeau (Jumu; Fig 3A). Chromatin immunoprecipitation and massively
121 parallel DNA sequencing (ChIP-seq) for Jumu in 0-24hr embryos was performed by the
122 modENCODE project (ENCSR946VDB)(Luo et al., 2020), which identified a Jumu binding
123 region that overlaps with the *bsd* core promoters (Fig. 3A). To understand if Jumu regulates
124 *bsd* expression, we optimized a quantitative real time PCR (qRT-PCR) strategy by testing the
125 expression of a known Jumu target gene, *heartless* (*htl*), in embryos homozygous for a strong
126 hypomorphic allele of *jumu*^{2.12} (Fig. 3B)(Ahmad et al., 2016). qRT-PCR showed that both *htl* and

127 *bsd* expression was significantly reduced in *jumu*^{2.12} embryos compared to controls (Fig. 3B). In
128 addition, *jumu*^{2.12} embryos showed muscle morphogenesis defects similar to *bsd*¹ embryos (Fig.
129 3C), and *slou>GFP* myotubes were short and incorrectly targeted in *jumu*^{2.12} embryos (Fig. 3D).
130 Our studies are consistent with a model in which Jumu directly activates *bsd* expression to
131 regulate myotube guidance and maintain muscle cell identity. Jumu also acts upstream of Polo
132 through an unknown mechanism to regulate cardiac muscle specification (Ahmad et al., 2012).
133 One exciting possibility is that Jumu transcriptionally activates *bsd* to regulate Polo activity.

134 The specification of thirty distinct founder cells (FCs) per hemisegment is accomplished
135 through morphogen-induced specification of equivalence groups, lateral inhibition within
136 equivalence groups to establish individual progenitors, and combinatorial expression of distinct
137 transcription factors to generate diverse cell identities. The final musculoskeletal pattern
138 however is established when FCs undergo a morphological transformation into myotubes, and
139 respond to navigational cues transduced by the transmembrane receptors Heartless, Kon-tiki,
140 and Robo to elongate and identify muscle attachment sites at the segment boundary (Kramer et
141 al., 2001; Schnorrer et al., 2007; Yang et al., 2020). The developmental mechanisms that direct
142 FC cell fate specification and morphogenesis are commonly used strategies that regulate
143 organogenesis across Metazoa, but FCs also employ a muscle-specific developmental
144 program, directional fusion, to generate multinucleate muscle cells with distinct identities. FCs
145 and myotubes only fuse with mononucleate fusion competent myoblasts (FCMs), but do not
146 fuse with each other (Fig. 1D)(Bothe and Baylies, 2016).

147 Directional fusion persists during myotube guidance through a Bsd-dependent
148 mechanism. Myotubes seeded from distinct FCs do not fuse with each other, but in *bsd* mutant
149 embryos the loss of directional fusion produced muscles with intermediate identities (Fig. 1D).
150 Directional fusion does not appear to be regulated by the position of the myotube in the
151 segment. *tum* and *htl* myotube leading edges navigate to incorrect positions, but do not fuse
152 with other myotubes (Fig. 2A)(Yang et al., 2020). These observations suggest Bsd prevents
153 myotube fusion by blocking the activity or function of pro-fusion pathways in maturing myotubes.
154 The nephrin-like transmembrane proteins Kirre and Sticks and stones (Sns) are differentially
155 expressed in muscle precursors: Kirre is expressed in FCs and Sns is expressed FCMs (Bour et
156 al., 2000; Ruiz-Gómez et al., 2000). Sns is a ligand of Kirre, and heterophilic interactions
157 between Kirre and Sns are thought to confer FC-FCM cell recognition, and provide the adhesive
158 forces necessary for fusion (Krauss, 2010). Homophilic interactions between Kirre expressing
159 cells in culture promotes cell-cell adhesion (Menon et al., 2005), suggesting enhanced
160 expression or activation of Kirre in myotubes could drive non-directional fusion. *kirre*

161 transcription is induced in visceral muscle cells by ERK signaling (Englund et al., 2003), and we
162 show Bsd negatively regulates ERK activation (Fig. 2C-F). It is possible that Bsd suppresses
163 Kirre activity to maintain directional fusion and preserve muscle cell identity. However, spatial
164 misexpression of Kirre in the somatic mesoderm alone is not sufficient to induce obvious non-
165 directional cell fusion (Menon et al., 2005), suggesting Bsd regulates multiple cell fusion
166 proteins.

167 The expression of regulatory kinases is spatially and temporally dynamic, and
168 approximately 50% of *Drosophila* kinases show tissue-specific expression during the late stages
169 of embryogenesis (Yang et al., 2022). Bsd expression follows this pattern, and is enriched in the
170 somatic mesoderm during myotube guidance (Yang et al., 2022). Htl is a receptor tyrosine
171 kinase that transduces FGF signals, and Htl is broadly expressed in the mesoderm after
172 gastrulation (Fisher et al., 2012). However, during organogenesis, *htl* expression is restricted to
173 a subset of progenitors that will give rise to cardiac, somatic, and visceral muscle (Yang et al.,
174 2020). We confirmed that Jumu regulates *htl* expression in Stage 12 embryos, and show Jumu
175 also regulates *bsd* expression (Fig. 3A,B). Jumu is expressed in FCs and, although repressors
176 have been identified that block *jumu* expression in FCMs, the mechanisms that directly activate
177 *jumu* expression in the mesoderm are unknown (Ahmad et al., 2012; Ciglar et al., 2014).
178 Nonetheless, our study shows that Jumu dictates the expression of at least two regulatory
179 kinases, Bsd and Htl, which argues only a small number of transcription factors may be needed
180 to establish the dynamic spatiotemporal expression of regulatory kinases that control cell
181 morphogenesis. Since zebrafish regulatory kinases also show dynamic expression patterns
182 (Yang et al., 2022), it will be important to understand how cell identity and the expression of
183 morphogenetic transcription factors like Jumu are coordinated to direct organogenesis across
184 Metazoa.

185 **Acknowledgements.** We thank Shaad Amhad (Indiana State University) for sending *jumu* flies,
186 and Frank Schnorrer (IBDM, Marseille, France) for providing *slou-mCD8-GFP* flies. We also
187 thank the larger *Drosophila* community for stocks and reagents, and Kevin White's laboratory for
188 performing the Jumu ChIP-seq. ANJ was supported by NIH R01AR070299.

189 **Author Contributions.** Conceptualization: S.Y. and A.N.J., Methodology: S.Y. and A.N.J.,
190 Formal analysis: S.Y. and A.N.J., Investigation: S.Y., Resources: A.N.J.; Data curation: S.Y.,
191 Writing original draft: S.Y. and A.N.J.

192 **Competing interests.** The authors declare no competing interests.

193 **Methods**

194 ***Drosophila* genetics**

195 The following stocks were obtained from the Bloomington Stock Center: *tum*^{DH15}, *P{GMR40D04-*
196 *GAL4}attP2* (*slou.Gal4*), and *P{GMR57C12-GAL4}attP2* (*nau.Gal4*). The other stocks used in
197 this study were *bsd*¹ (Yang et al., 2022), *jumu*^{2.12} (Ahmad et al., 2012), and *P{slou-mCD8-GFP}*
198 (*Schnorrer et al.*, 2007). *Cyo*, *P{Gal4-Twi}*, *P{2X-UAS.eGFP}*; *Cyo*, *P{wg.lacZ}*; *TM3*, *P{Gal4-*
199 *Twi}*, *P{2X-UAS.eGFP}*; and *TM3*, *P{ftz.lacZ}* balancers were used to genotype embryos.

200 **Immunohistochemistry**

201 Antibodies used were α -Mef2 (1:1000, gift from R. Cripps), α -Tropomyosin (1:600, Abcam,
202 MAC141), α -GFP (1:600, Torrey Pines Biolabs, TP-401), and α -dpERK (1:300, Cell Signaling
203 Technologies, 4377). Embryo antibody staining was performed as described (Johnson et al.,
204 2013); HRP-conjugated secondary antibodies in conjunction with the TSA system (Molecular
205 Probes) were used to detect primary antibodies.

206 **Imaging and image quantification**

207 Embryos were imaged with a Zeiss LSM800 confocal microscope. For time-lapse imaging,
208 dechorionated St12 embryos were mounted in halocarbon oil and scanned at 6min intervals.
209 Control and mutant embryos were prepared and imaged in parallel where possible, and imaging
210 parameters were maintained between genotypes. Fluorescent intensity and cell morphology
211 measurements were made with ImageJ software.

212 **Phenotypic scoring, analysis, and visualization**

213 Each embryonic hemisegment has 30 distinct muscles with a fixed pattern as shown in Figure
214 1A. Muscle phenotypes were analyzed in hemisegments A2-A7, in a minimum of nine embryos
215 per genotype. A Tropomyosin antibody was used to visualize all body wall muscles, and the
216 percent defective was calculated for each of the 30 muscles in minimum of 42 hemisegments
217 from seven different embryos. $\% \text{ Defective} = \# \text{ of abnormal muscles/hemisegments scored}$. To
218 visualize affected muscles, percent defective was converted to a schematic heat map on the
219 body wall muscle pattern.

220 **Immunoprecipitation and Western blotting**

221 For *Drosophila* proteins, S2 cells (8×10^6) were transfected with 1.5 μ g of pAMW.Bsd or pAMW
222 plasmids in 6-well plates. Cells were cultured for 24h collected, washed twice with PBS, lysed
223 with 600 μ l IP buffer (20 mM Hepes, pH=7.4, 150 nM NaCl, 1% NP40, 1.5 mM MgCl₂, 2 mM
224 EGTA, 10 mM NaF, 1 mM Na₃VO₄, 1X proteinase inhibitor), incubated on ice for 30 min,
225 centrifuged at 12000Xg for 15min. The supernatant was collected, and Western blots were
226 performed by standard method using precast gels (#456-1096, BioRad), and imaged with the

227 ChemiDoc XRS+ system (BioRad). Antibodies used for Western blots were α -dpERK (1:1000,
228 Cell Signaling Technologies, 4377), α -ERK (1:1000, Enzo Life Sciences, ADI-KAP-MA001), and
229 α -Myc (1:1000, Sigma, PLA0001).

230 **Quantitative real time PCR**

231 Total RNA was extracted with RNeasy mini kit (74104, Qiagen), and quantified (Nanodrop
232 2000). cDNA was prepared by reverse transcription with M-MLV Reverse Transcriptase
233 (28025013, Thermo) with 2000ng RNA. PowerUp Sybr Green Master Mix (A25742, Thermo)
234 and ABI StepOne system (Applied Biosystems) were used for quantitative RT-PCR.
235 Quantification was normalized to *GAPDH* or *RpL32*. Primers used:

236 Htl-F-5`-ACCAAATTGCCAGAGGAATG-3`

237 Htl-R-5`-GGTAGCCTGCCATTTGTGTT-3`

238 Bsd-F-5`-TCAACGCTAAGCACTCCGTT-3`

239 Bsd-R-5`-CGCCTCTGCTCCATGTCTAG-3`

240 Rp32-F-5`-ATGCTAAGCTGTGCGACAAATG-3`

241 Rp32-R-5`-GTTCGATCCGATACCGATGT-3`

242 **Bioinformatic and statistical analysis**

243 DNAMAN (Lynnon Biosoft, Ver. 10) was used to identify consensus transcription factor binding
244 sites. Statistical analyses were performed with GraphPad Prism 9 software, and significance
245 was determined with the unpaired student's t-test, and two-sided Fisher's exact test. Sample
246 sizes are indicated in the figure legends. All individuals were included in data analysis.

References

- Ahmad, S.M., Bhattacharyya, P., Jeffries, N., Gisselbrecht, S.S., Michelson, A.M., 2016. Two Forkhead transcription factors regulate cardiac progenitor specification by controlling the expression of receptors of the fibroblast growth factor and Wnt signaling pathways. *Development* 143, 306-317.
- Ahmad, Shaad M., Tansey, Terese R., Busser, Brian W., Nolte, Michael T., Jeffries, N., Gisselbrecht, Stephen S., Rusan, Nasser M., Michelson, Alan M., 2012. Two Forkhead Transcription Factors Regulate the Division of Cardiac Progenitor Cells by a Polo-Dependent Pathway. *Developmental Cell* 23, 97-111.
- Balsalobre, A., Drouin, J., 2022. Pioneer factors as master regulators of the epigenome and cell fate. *Nature reviews. Molecular cell biology* 23, 449-464.
- Bothe, I., Baylies, M.K., 2016. Drosophila myogenesis. *Current biology : CB* 26, R786-791.
- Bour, B.A., Chakravarti, M., West, J.M., Abmayr, S.M., 2000. Drosophila SNS, a member of the immunoglobulin superfamily that is essential for myoblast fusion. *Genes Dev* 14, 1498-1511.
- Carmena, A., Gisselbrecht, S., Harrison, J., Jiménez, F., Michelson, A.M., 1998. Combinatorial signaling codes for the progressive determination of cell fates in the Drosophila embryonic mesoderm. *Genes & Development* 12, 3910-3922.
- Ciglar, L., Girardot, C., Wilczyński, B., Braun, M., Furlong, E.E.M., 2014. Coordinated repression and activation of two transcriptional programs stabilizes cell fate during myogenesis. *Development* 141, 2633-2643.
- D'Avino, P.P., Savoian, M.S., Capalbo, L., Glover, D.M., 2006. RacGAP50C is sufficient to signal cleavage furrow formation during cytokinesis. *Journal of Cell Science* 119, 4402-4408.
- de Jossineau, C., Bataillé, L., Jagla, T., Jagla, K., 2012. Diversification of muscle types in Drosophila: upstream and downstream of identity genes. *Current topics in developmental biology* 98, 277-301.
- Ebrahimi, S., Fraval, H., Murray, M., Saint, R., Gregory, S.L., 2010. Polo kinase interacts with RacGAP50C and is required to localize the cytokinesis initiation complex. *Journal of Biological Chemistry* 285, 28667-28673.
- Englund, C., Lorén, C.E., Grabbe, C., Varshney, G.K., Deleuil, F., Hallberg, B., Palmer, R.H., 2003. Jeb signals through the Alk receptor tyrosine kinase to drive visceral muscle fusion. *Nature* 425, 512-516.
- Fisher, B., Weiszmann, R., Frise, E., Hammonds, A., Tomancak, P., Beaton, A., Berman, B., Quan, E., Shu, S., Lewis, S., Rubin, G., Barale, C., Laguetas, E., Quinn, J., Ghosh, A., Hartenstein, V., Ashburner, M., Celniker, S., 2012. BDGP website. <https://insitu.fruitfly.org/cgi-bin/ex/insitu.pl>.
- Gregory, S.L., Ebrahimi, S., Milverton, J., Jones, W.M., Bejsovec, A., Saint, R., 2008. Cell division requires a direct link between microtubule-bound RacGAP and Anillin in the contractile ring. *Current Biology* 18, 25-29.
- Guerin, C.M., Kramer, S.G., 2009. RacGAP50C directs perinuclear gamma-tubulin localization to organize the uniform microtubule array required for Drosophila myotube extension. *Development* 136, 1411-1421.
- Hao, Y., Jin, L.H., 2017. Dual role for Jumu in the control of hematopoietic progenitors in the Drosophila lymph gland. *eLife* 6.
- Johnson, A.N., Mokalled, M.H., Valera, J.M., Poss, K.D., Olson, E.N., 2013. Post-transcriptional regulation of myotube elongation and myogenesis by Hoi Polloi. *Development* 140, 3645-3656.
- Kang, T.H., Kim, K.T., 2006. Negative regulation of ERK activity by VRK3-mediated activation of VHR phosphatase. *Nature cell biology* 8, 863-869.
- Kang, T.H., Kim, K.T., 2008. VRK3-mediated inactivation of ERK signaling in adult and embryonic rodent tissues. *Biochimica et biophysica acta* 1783, 49-58.
- Kramer, S.G., Kidd, T., Simpson, J.H., Goodman, C.S., 2001. Switching repulsion to attraction: changing responses to slit during transition in mesoderm migration. *Science (New York, N.Y.)* 292, 737-740.
- Krauss, R.S., 2010. Regulation of promyogenic signal transduction by cell-cell contact and adhesion. *Experimental Cell Research* 316, 3042-3049.
- Luo, Y., Hitz, B.C., Gabdank, I., Hilton, J.A., Kagda, M.S., Lam, B., Myers, Z., Sud, P., Jou, J., Lin, K., Baymuradov, U.K., Graham, K., Litton, C., Miyasato, S.R., Strattan, J.S., Jolanki, O., Lee, J.W., Tanaka, F.Y., Adenekan, P., O'Neill, E., Cherry, J.M., 2020. New developments on the Encyclopedia of DNA Elements (ENCODE) data portal. *Nucleic acids research* 48, D882-d889.

- McAdow, J., Yang, S., Ou, T., Huang, G., Dobb, M.B., Gurnett, C.A., Johnson, A.N., 2022. A pathogenic mechanism associated with myopathies and structural birth defects involves TPM2 directed myogenesis. *JCI Insights* 7, e152466.
- Menon, S.D., Osman, Z., Chenchill, K., Chia, W., 2005. A positive feedback loop between Dumbfounded and Rolling pebbles leads to myotube enlargement in *Drosophila*. *Journal of Cell Biology* 169, 909-920.
- Peter, I.S., Davidson, E.H., 2016. Chapter Thirteen - Implications of Developmental Gene Regulatory Networks Inside and Outside Developmental Biology, in: Wassarman, P.M. (Ed.), *Current topics in developmental biology*. Academic Press, pp. 237-251.
- Ruiz-Gómez, M., Coutts, N., Price, A., Taylor, M.V., Bate, M., 2000. *Drosophila dumbfounded*: a myoblast attractant essential for fusion. *Cell* 102, 189-198.
- Sandmann, T., Jensen, L.J., Jakobsen, J.S., Karzynski, M.M., Eichenlaub, M.P., Bork, P., Furlong, E.E.M., 2006. A Temporal Map of Transcription Factor Activity: Mef2 Directly Regulates Target Genes at All Stages of Muscle Development. *Developmental Cell* 10, 797-807.
- Schnorrer, F., Kalchauer, I., Dickson, B.J., 2007. The transmembrane protein Kon-tiki couples to Dgrip to mediate myotube targeting in *Drosophila*. *Dev Cell* 12, 751-766.
- Somers, W.G., Saint, R., 2003. A RhoGEF and Rho family GTPase-activating protein complex links the contractile ring to cortical microtubules at the onset of cytokinesis. *Developmental cell* 4, 29-39.
- Yang, S., McAdow, J., Du, Y., Trigg, J., Taghert, P., Johnson, A.N., 2022. Spatiotemporal expression of regulatory kinases directs the transition from mitotic growth to cellular morphogenesis. *Nat Commun* 13, 772.
- Yang, S., Weske, A., Du, Y., Valera, J.M., Jones, K.L., Johnson, A.N., 2020. FGF signaling directs myotube guidance by regulating Rac activity. *Development* 147, dev183624.

Figure 1. Bsd maintains directional fusion and muscle identity.

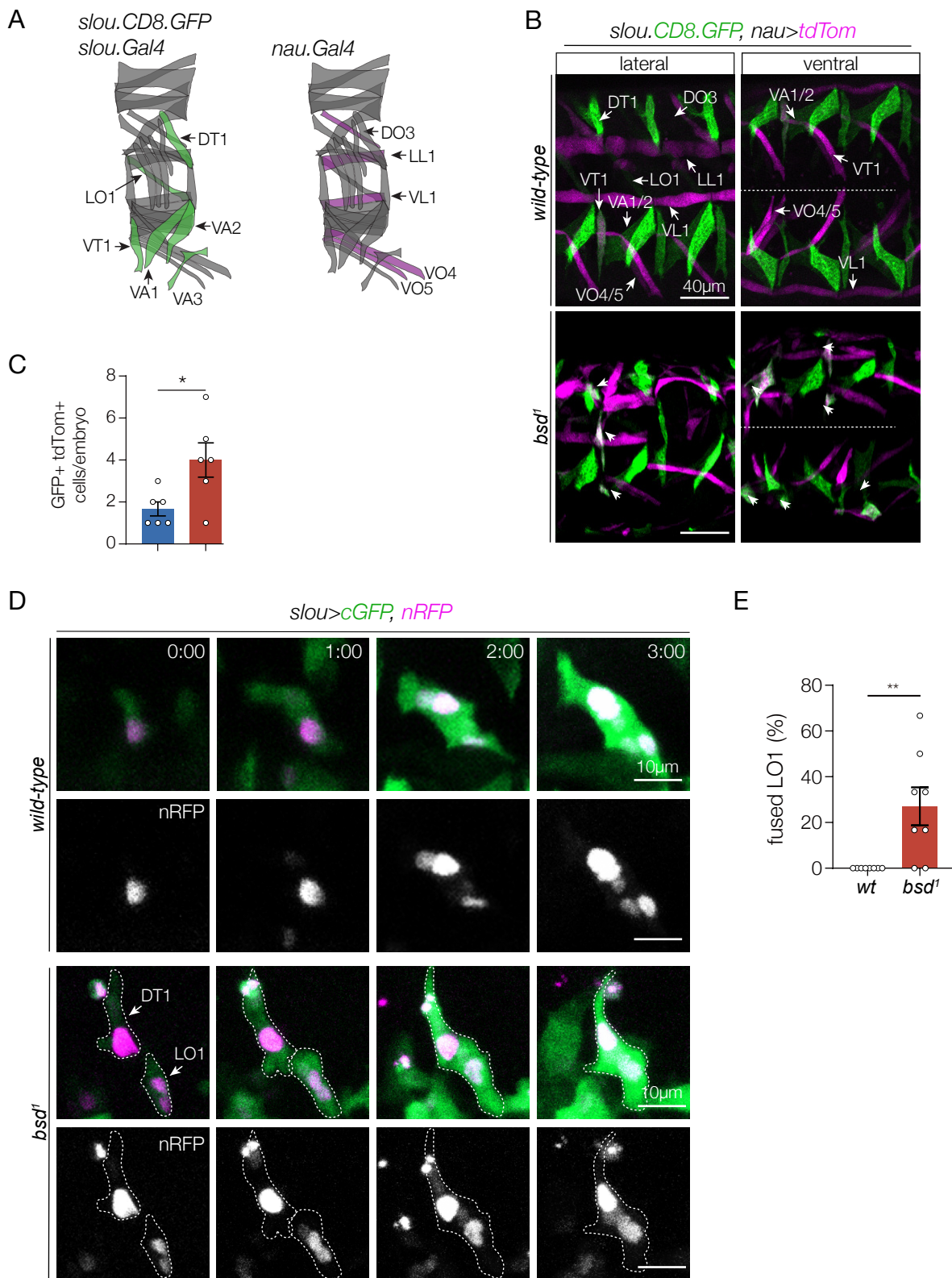


Figure 1. Bsd maintains directional fusion and muscle identity. (A) Diagrams of the stereotypic pattern of body wall muscles in one hemisegment. Each muscle expresses a unique combination of identity genes, including *slouch* (*slou*) and *nautilus* (*nau*). *slou* transgenes are active in Doral Transverse 1 (DT1), Longitudinal Oblique (LO1), Ventral Acute 1-3 (VA1-3), and the Ventral Transverse 1 (VT1) muscles (green). A *nau* transgene is active in the Dorsal Oblique 3 (DO3), Longitudinal Lateral 1 (LL1), Ventral Lateral 1 (VL1), and Ventral Oblique 4-5 (VO4-5) muscles (violet). (B) *bsd*¹ myotubes show intermediate identities. Confocal micrographs of live Stage 16 embryos imaged for *slou-CD8-GFP* (green) and *nau>tdTom* (violet). *slou-CD8-GFP* and *nau.Gal4>tdTom* are active in largely non-overlapping populations of body wall muscles in wild-type embryos, although VT1 occasionally co-expressed GFP and tdTom. *bsd*¹ embryos had more muscles that co-expressed GFP and tdTom than wild-type embryos (arrowheads). (C) Quantification of GFP/tdTom double positive cells. The number of double positive cells in hemisegments A2-A7 is shown; each data point represents one embryo. (D) *bsd*¹ myotubes undergo non-directional fusion. Live imaging stills of LO1 myotubes in Stage 12-15 embryos that expressed cytoplasmic GFP (green) and nuclear RFP (violet) under the control of *slou.Gal4*. Live imaging initiated when GFP fluorescence was detectable in LO1 myotubes (0:00). Control myotubes elongate in a stereotypical fashion and identify attachment sites to acquire an oblique morphology. Notice the number of LO1 myonuclei increases due to directional fusion. *bsd*¹ LO1 myotubes often fused with DT1 myotubes and the LO1-DT1 muscle acquired a transverse morphology. (E) Quantification of non-directional myotube fusion from live imaging. The number of LO1 fusion events with other *slou>GFP* myotubes in hemisegments A2-A7 is shown; each data point represents one embryo. Significance in (C,E) was determined by unpaired students t-test. Error bars represent SEM. (*) p<0.05, (**) p<0.01. (###) hr:min.

Figure 2 Bsd regulates MAPK activity

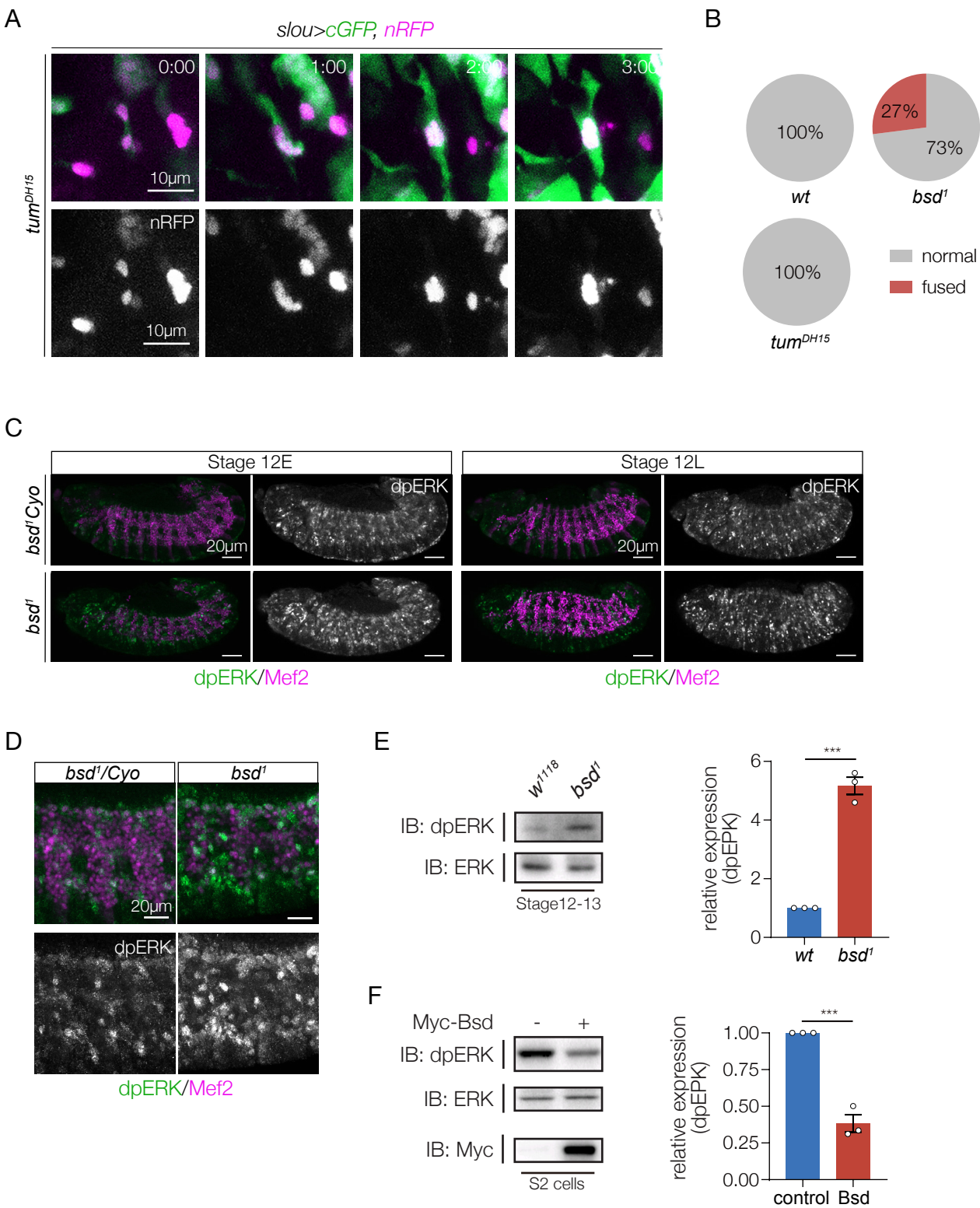
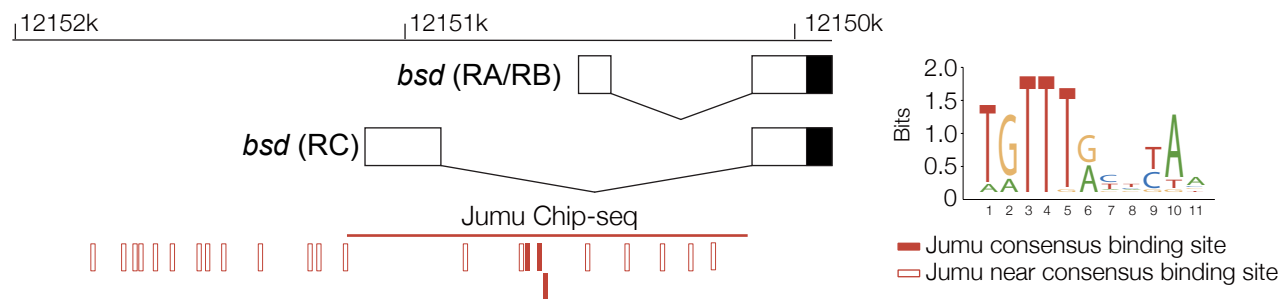


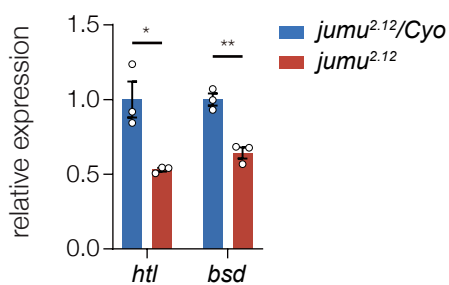
Figure 2. Bsd regulates ERK activity. (A) Tum does not regulate directional fusion. Live imaging stills of LO1 myotubes in Stage 12-15 embryos as described in Fig. 1. *tum*^{DH15} LO1 myotubes showed severe guidance defects, but did not fuse with other *slou>GFP* myotubes. (B) Quantification of non-directional myotube fusion from live imaging. n≥6 embryos per genotype. (C,D) Bsd represses ERK phosphorylation. Stage 12 embryos labeled for dpERK (green) and Mef2 (violet). dpERK identifies cells with activated ERK and Mef2 is expressed in all myogenic cells. *bsd*¹ embryos showed more dpERK in the mesoderm than controls. High magnification confocal micrographs of the embryos in (C) are shown in (D). (St12E) Stage 12 early, (St12L) Stage 12 late. (E) Stage 12 embryo lysates immunoblotted with dpERK. *bsd*¹ embryo lysates showed significantly more phosphorylated ERK than controls. (F) Cells transfected with Bsd showed significantly less phosphorylated ERK than controls. Lysates from S2 cells transfected with Bsd.Myc and control plasmids were immunoblotted with dpERK and Myc to detect transgenic proteins. Data points in the dpERK quantifications (E,F) represent one biological replicate. Significance was determined by unpaired students t-test. Error bars represent SEM. (***) p<0.001.

Figure 3 Jumu activates *bsd* expression

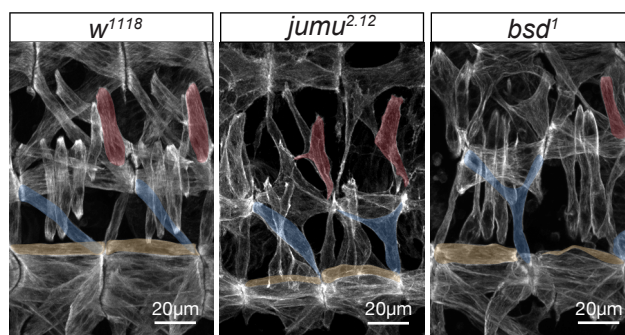
A



B



C



D

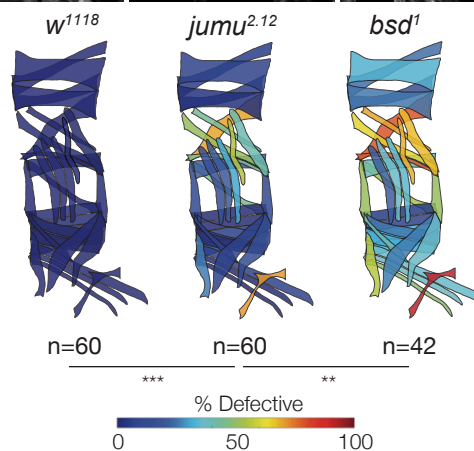
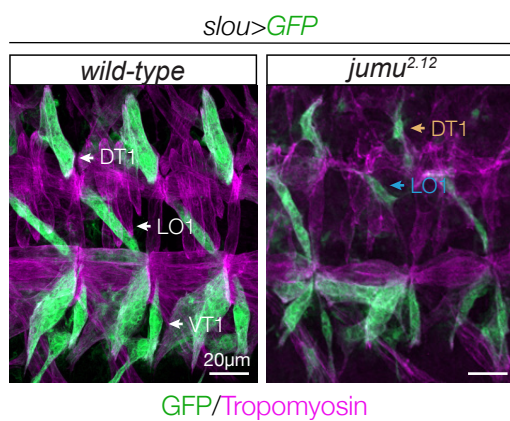


Figure 3. Jumu activates *bsd* expression. (A) Diagram of the *bsd* core promoter region. Open boxes represent untranslated regions; shaded boxes show the beginning of the open reading frame. Molecular coordinates refer to chromosome 2R. The consensus Jumu binding site was reported in (Hao and Jin, 2017). The ChIP-seq binding region was reported by modENCODE project (ENCSR946VDB). (B) Quantitative real time PCR analysis of *htl* and *bsd* mRNA showed each transcript was reduced in Stage 12 *jumu* embryo lysates (n=3 biological replicates). (C) Muscle phenotypes in *jumu*^{2.12} and *bsd*¹ embryos. Stage 16 embryos labeled with Tropomyosin. DT1, LO1, and VL1 muscles are pseudocolored red, blue, and yellow. Muscle morphology defects was comparable between *jumu*^{2.12} and *bsd*¹ embryos. Quantification of muscle phenotypes. Muscles were scored in hemisegments A2-A7 of St16 embryos. Abnormal phenotypes (missing muscles, muscles with attachment site defects, and muscles that failed to elongate) were scored “defective”. The frequencies of muscle defects are shown as a heat map on the stereotypic muscle pattern in one embryonic hemisegment. (n) number of hemisegments scored. (D) *jumu*^{2.12} DT1, LO1, and VT1 muscle phenotypes. Stage 16 embryos labeled for *slou>GFP* (green) and Tropomyosin (violet). *jumu*^{2.12} muscles had attachment site defects (orange and blue arrows). Significance was determined by unpaired students t-test (B) or Fisher’s exact test (C). Error bars represent SEM. (*) p<0.05, (**) p<0.01, (***) p<0.001.

Movie Captions.

Supplementary Movie 1. Bsd prevents non-directional fusion. Live imaging of LO1 myotubes from Stage 12 *slou>eGFP,nRFP* embryos. *slou> eGFP* (green) myotubes fused in *bsd*¹ embryos but not controls. The number of nRFP positive myonuclei (violet) increased due to directional fusion between myotubes and fusion competent myoblasts.

Supplementary Movie 2. Tum does not regulate myotube fusion. Live imaging of LO1 myotubes from Stage 12 *tum*^{DH15} *slou>eGFP,nRFP* embryos. *slou> eGFP* (green) myotubes did not fuse in *tum*^{DH15} embryos. Interestingly, the myonuclei (violet) remained clustered in mutant myotubes.